



LAWRENCE
LIVERMORE
NATIONAL
LABORATORY

MHD Simulations of Core Collapse Supernovae with Cosmos++

S. Akiyama, J. Salmonson

July 12, 2010

Deciphering the Ancient Universe with Gamma-ray Bursts"
Kyoto, Japan
April 19, 2010 through April 23, 2010

Disclaimer

This document was prepared as an account of work sponsored by an agency of the United States government. Neither the United States government nor Lawrence Livermore National Security, LLC, nor any of their employees makes any warranty, expressed or implied, or assumes any legal liability or responsibility for the accuracy, completeness, or usefulness of any information, apparatus, product, or process disclosed, or represents that its use would not infringe privately owned rights. Reference herein to any specific commercial product, process, or service by trade name, trademark, manufacturer, or otherwise does not necessarily constitute or imply its endorsement, recommendation, or favoring by the United States government or Lawrence Livermore National Security, LLC. The views and opinions of authors expressed herein do not necessarily state or reflect those of the United States government or Lawrence Livermore National Security, LLC, and shall not be used for advertising or product endorsement purposes.

MHD Simulations of Core Collapse Supernovae with Cosmos++

Shizuka Akiyama* and Jay Salmonson†

**shizuka@slac.stanford.edu*

†*salmonson1@llnl.gov*

Abstract.

We performed 2D, axisymmetric, MHD simulations with Cosmos++ in order to examine the growth of the magnetorotational instability (MRI) in core-collapse supernovae. We have initialized a non-rotating $15 M_{\odot}$ progenitor, infused with differential rotation and poloidal magnetic fields. The collapse of the iron core is simulated with the Shen EOS, and the parametric Ye and entropy evolution. The wavelength of the unstable mode in the post-collapse environment is expected to be only ~ 200 m. In order to achieve the fine spatial resolution requirement, we employed remapping technique after the iron core has collapsed and bounced.

The MRI unstable region appears near the equator and angular momentum and entropy are transported outward. Higher resolution remap run display more vigorous overturns and stronger transport of angular momentum and entropy. Our results are in agreement with the earlier work by Akiyama et al. [1] and Obergaulinger et al. [2].

Keywords: MHD, Numerical Simulations, Core Collapse Supernova, MRI

PACS: 90

INTRODUCTION

Neutron stars are spinning and magnetized, and magnetars are the extreme neutron stars with magnetic fields $> 10^{14}$ G. The GRBs associated with ultra-relativistic outflow are considered to be generated by the MHD jets from the rotating, magnetized engine; the so-called "Collapsar" or magnetar. The close association of those objects to core-collapse supernovae leads to the question whether supernova explosions, too, are involved with rotation and magnetic fields. If it is the case for most core collapse supernovae, the modest initial magnetic fields have to be amplified more efficiently than linear wrapping of the field lines or compression. Akiyama et al. [1] pointed out that the core collapse environment is naturally unstable to the magnetorotational instability (MRI) [3], which amplifies magnetic fields exponentially in linear regime. Their 1D study indicated that a small seed field in the iron core is amplified to $\sim 10^{15-17}$ G within tens of milliseconds after bounce. This prediction has to be verified in numerical simulations because of the highly non-linear nature of the problem.

NUMERICAL MODELS AND METHOD

The collapse of iron core is simulated by 2D, axisymmetric, MHD simulations using Cosmos++ code. Cosmos++ is a multidimensional, massively parallel, Newtonian and

fully general relativistic radiation-magneto-hydrodynamical code [4]. We begin with a non-rotating $15 M_{\odot}$ progenitor model, s15s2b7 [5]. For rotation, we employ constant angular momentum profile: $\Omega(r) = \Omega_0 \frac{R^2}{r^2 + R^2}$, where Ω_0 is the initial central angular velocity, and R determines the degree of differential rotation. Magnetic field is obtained by taking curl of the magnetic potential due to a current loop with a radius D [6]. The peak of the magnetic field is set to a magnetic field strength B_0 . We present a model with $\Omega_0 = 2.0$ [rad/s], $R = 850$ km, $D = 400$ km, and $B_0 = 10^{12}$ G.

The collapse of the initial iron core is simulated using the realistic nuclear Shen EOS [7], and the electron fraction (Ye) and entropy evolution following the parametrization of neutrino physics by Liebendörfer [8]. We neglect neutrino transport, and we plan such improvement to future work.

The wavelength of the unstable mode is directly proportional to the magnetic field strength. Taking a conservative case, for the typical pulsar field strength $\sim 10^{12}$ G, the most unstable wavelength is $\sim 0.18 km (\frac{B}{10^{12} [G]})(\frac{1000 [rad/s]}{\Omega})(\frac{10^{13}}{\rho [g/cm^3]})^{0.5}$. By giving 10 grid zones per wavelength to resolve the MRI growth, ~ 20 m resolution is required to cover between ~ 10 – $\text{few} \times 100$ km in the post-collapse environment. It is unrealistic to simulate the iron core collapse with such a fine spatial resolution. Therefore, we first simulate the collapse of the iron core with $n_r = 256$ and $n_{\theta} = 64$, and $0 < \text{radius} < 6,800$ km and $0 < \theta < \frac{\pi}{2}$ (base simulation). The smallest radial resolution in the base simulation was ~ 300 m. At 30 msec after the core bounce in the base simulation, we remap the profiles to a new mesh with $n_r = 1024$ or 2048 and $n_{\theta} = 1024$ or 2048 (std or stdx2 run), and $12 < \text{radius} < 68$ km and $\frac{\pi}{6} < \theta < \frac{5\pi}{6}$. The smallest spatial resolution was 11 and 5.5 m respectively for std and stdx2 runs.

RESULTS

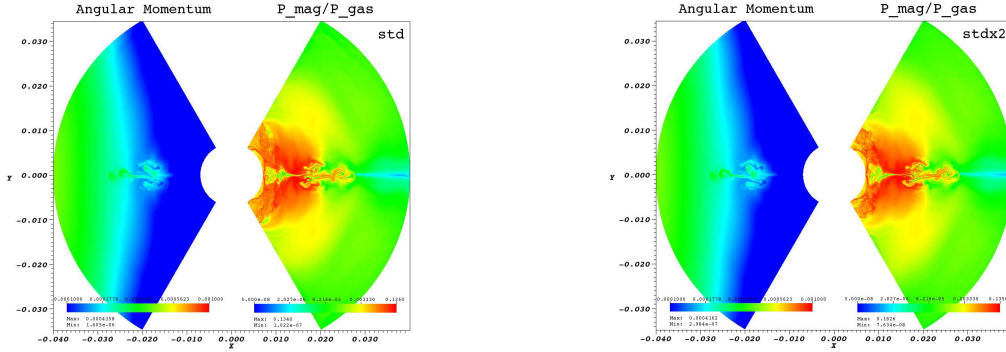


FIGURE 1. Angular momentum and ratio between magnetic pressure and gas pressure for std (left panel) and stdx2 (right panel) runs at 9 msec after remapping. The simulated region is $12 - 68$ km in radius and $0 - \frac{\pi}{2}$ in θ .

After the iron core collapsed, its initial magnetic fields were amplified up to $\sim 10^{15}$ G, and the core was spun up to ~ 2000 [rad/s]. At the time of remapping, the most unstable wavelength of the MRI were few km. The resolution obtained by both std and stdx2 runs are sufficient to resolve the MRI growth. Indeed, during the first 9 msec after the

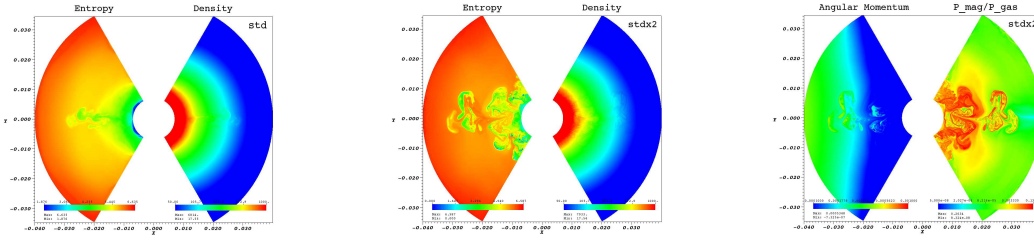


FIGURE 2. Entropy and mass density for std (left) and stdx2 (middle) runs at 15 msec after remapping. The right panel is the same with Figure 1 for stdx2 run at 15 msec after remapping.

remapping, the evolution of std and stdx2 runs are very similar (Figure 1). In both runs, the MRI unstable region appears near the equatorial region, and magnetic bubbles rises in the cylindrical radius direction, instead of spherical radius direction. At 15 msec after the remapping, the two runs shows differences (Figure 2); higher resolution run (stdx2) display more vigorous overturns and stronger outward transport of entropy and angular momentum. The MRI unstable region kept filling up the simulated area until the end of the std run (45 msec).

Our results confirm that the MRI is unstable in the core collapse environment. The qualitative results presented here are also in agreement with Akiyama et al. [1] and Obergaulinger et al. [2]. It is noted that the additional mixing of entropy caused by magnetic instability may affect the neutrino emission opacity. This point should be further investigated with future simulations with neutrino transport.

ACKNOWLEDGMENTS

S. A. is supported by grants from the Kavli Institute for Particle Astrophysics and Cosmology (KIPAC) through a SciDAC Postdoctoral Fellowship. S. A. and J. S. thank Christian D. Ott for providing the Shen EOS table.

REFERENCES

1. S. Akiyama, J. C. Wheeler, D. L. Meier, and I. Lichtenstadt, *Astrophysical Journal* **584**, 954 (2003).
2. M. Obergaulinger, P. Cerdá-Durán, E. Müller, and M. A. Aloy, *Astronomy and Astrophysics* **498**, 241 (2009).
3. S. A. Balbus, and J. F. Hawley, *Astrophysical Journal* **376**, 214–233 (1991).
4. P. Anninos, P. C. Fragile, and J. D. Salmonson, *Astrophysical Journal* **635**, 723 (2005).
5. S. E. Woosley, and T. A. Weaver, *Astrophysical Journal Supplement Series* **101**, 181 (1995).
6. J. D. Jackson, *Classical Electrodynamics*, Wiley, NY, 1975, second edn.
7. H. Shen, H. Toki, K. Oyamatsu, and K. Sumiyoshi, *Nuclear Physics A* **637**, 435 (1998).
8. M. Liebendörfer, *Astrophysical Journal* **633**, 1042 (2005).

This work performed under the auspices of the U.S. Department of Energy by Lawrence Livermore National Laboratory under Contract DE-AC52-07NA27344.